Evidence for a reorientation transition in the phase behaviour of a two-dimensional dipolar antiferromagnet

2004 J. Phys.: Condens. Matter 16 941

(http://iopscience.iop.org/0953-8984/16/6/021)

INSTITUTE OF PHYSICS PUBLISHING JOURNAL OF PHYSICS: CONDENSED MATTER

J. Phys.: Condens. Matter **16** (2004) 941–954 PII: S0953-8984(04)65194-0

Evidence for a reorientation transition in the phase behaviour of a two-dimensional dipolar antiferromagnet

A M Abu-Labdeh[1], J P Whitehead[1,4], K De'Bell[2] and A B MacIsaac[3]

[1] Department of Physics and Physical Oceanography, Memorial University of Newfoundland, Saint John's, Newfoundland, A1B 3X7, Canada
[2] Department of Mathematical Sciences, University of New Brunswick at Saint John, Saint John, New Brunswick, E2L 4L5, Canada
[3] Department of Applied Mathematics, University of Western Ontario, London, ON, N6A 5B9, Canada

Received 23 June 2003
Published 30 January 2004
Online at stacks.iop.org/JPhysCM/16/941 (DOI: 10.1088/0953-8984/16/6/021)

Abstract

The results from a series of Monte Carlo simulations are presented for the two-dimensional Heisenberg model consisting of classical spin vectors arranged on the vertices of a square lattice in which the spins interact through an antiferromagnetic exchange interaction, a magnetic surface anisotropy and the dipolar interaction. The simulations focus on the exchange dominated regime in which the strength of the exchange interaction is significantly greater than both the dipolar interaction and the magnetic surface anisotropy. The results from the simulations show that there exists a range of the magnetic surface anisotropy parameter values in which the system exhibits a reorientation transition from a planar antiferromagnetic phase at low temperature to a perpendicular antiferromagnetic phase at higher temperature. The phase diagram, obtained from the Monte Carlo calculations, is determined as a function of both temperature and magnetic surface anisotropy parameter for a fixed value of the exchange constant. In addition, the low temperature magnetization data suggests a softening of a spin wave stiffness close to the phase boundary between the two ordered states.

1. Introduction

Interest in low dimensional magnetic systems has grown considerably in recent years. One important class of reduced dimensional systems is ultra-thin magnetic films (UTMFs), which consist of several monolayers of magnetic atoms deposited on a non-magnetic substrate. The increased scientific interest in these materials is a consequence of advances in film fabrication

[4] Author to whom any correspondence should be addressed.

and characterization techniques. In addition to the scientific interest, these materials are also of potential technological importance in data storage and processing [1]. Of particular interest in the context of the current work is the use of antiferromagnetic films, which are used in the construction of spin valves [2].

Another class of reduced dimensional magnetic system of increasing scientific and technological interest is micromagnetic arrays which consist of high density arrays of nanomagnetic dots deposited on a non-magnetic substrate. Such systems can be fabricated to have a wide variety of structures [3, 4] and properties [5] that can be tuned in a continuous manner to give a variety of phase behaviour.

The results obtained from studies on low dimensional magnetic systems are also relevant to certain layered compounds that contain weakly interacting planes of magnetic ions. One important recent example of such compounds is the class of rare-earth superconductors, such as $REBa_2Cu_3O_{7-\delta}$ (RE = rare earth). Several of these compounds exhibit an antiferromagnetic ordering of the rare earth ions at low temperature [6]. While experimental determination of the effective dimensionality of these compounds is difficult they nevertheless exhibit certain behaviours characteristic of two dimensional magnetic systems close to the Néel temperature [7–10].

The wide range of phenomena that have been observed or predicted in these low dimensional magnetic materials arises from the complex interplay between three fundamental interactions: the exchange interaction, the magnetic surface anisotropy, and the dipolar interaction. A model that includes these three interactions may be described in terms of an energy E given by

$$E = g\sum_{i\neq j}\left(\frac{\vec{\sigma}_i\cdot\vec{\sigma}_j}{r_{ij}^3} - 3\frac{(\vec{\sigma}_i\cdot\vec{r}_{ij})(\vec{\sigma}_j\cdot\vec{r}_{ij})}{r_{ij}^5}\right) - J\sum_{\langle i,j\rangle}\vec{\sigma}_i\cdot\vec{\sigma}_j - \kappa\sum_i(\sigma_i^z)^2. \quad (1)$$

The first term denotes the dipolar interaction, the second the exchange interaction and the third the magnetic surface anisotropy. In this study we treat the spins as classical vectors of fixed magnitude and hence $\{\vec{\sigma}_i\}$ denotes a set of three dimensional vectors of unit magnitude.

The magnetic properties of UTMFs differ significantly from those of bulk materials in part because the isotropic exchange interaction cannot of itself sustain long-range magnetic order in these low dimensional materials. Of particular importance is the anisotropic and long range dipolar interaction, which plays a critical role in determining the magnetic properties of these materials. In the case of the planar ferromagnet the long range character of the dipolar interaction gives rise to a non-analytic contribution in the magnetic propagator. This modifies the spin wave spectra in the planar ferromagnet in the long wavelength limit such that $\lim_{q\to 0}\omega(q) \approx \sqrt{q}$. This modification of the spin wave spectra is sufficient to render the thermal spin wave fluctuations finite and hence allow for the appearance of long range magnetic order at finite temperature [11]. The dipolar interaction also plays an important role in the case of the uniaxial ferromagnetic Ising model, in which the spins are aligned perpendicular to the surface. In this case the interplay between the short range ferromagnetic exchange interaction and the long range antiferromagnetic dipolar interaction destabilizes the ferromagnetic ground state in favour of a striped phase [12–14]. This has been observed experimentally [16, 15].

The region separating the planar ferromagnetic phase and the uniaxial striped phase is determined by the asymmetry between the in-plane and out-of-plane spin alignment that arises from the combined effect of the magnetic surface anisotropy and the dipolar interaction. The analysis of this region is complicated by the inhomogeneous character of the striped phase and the complexities that arise from the dipolar interaction. Analytical and simulation studies do however show that the temperature dependent renormalization of these interactions, due to the

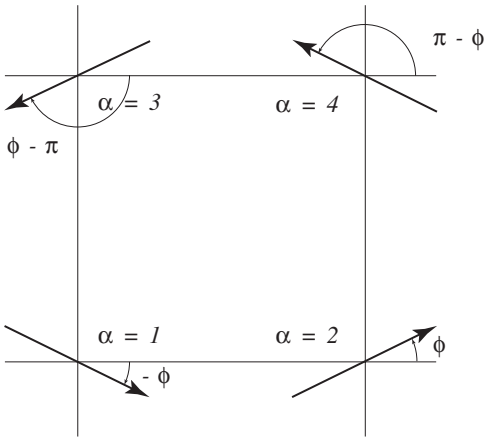

Figure 1. Definition of the angle ϕ characterizing the ground state spin configurations for the pure dipolar system.

thermal spin fluctuations, can give rise to a reorientation transition whereby the magnetization axis switches from in-plane to out-of-plane with changing temperature [17–20][5].

While ferromagnetic ($J > 0$) UTMFs have been studied extensively, less work has been done on antiferromagnetic ($J < 0$) UTMFs. However, the complex interplay between the exchange, magnetic surface anisotropy and dipolar interaction appears to provide an equally fascinating range of phenomena in the antiferromagnetic case.

In the case of the pure dipolar system ($J = 0$, $\kappa = 0$) the ground state for the square lattice is a planar antiferromagnetic state. Surprisingly, despite the anisotropic character of the dipolar interaction, the ground state of the square lattice is continuously degenerate [21, 22], a fact that had been noted earlier for the honeycomb lattice [23]. The spin configurations that comprise this ground state manifold are described in terms of a magnetic sublattice consisting of four lattice sites, with the spin at each lattice site oriented as shown in figure 1 [21]. Each ground state is characterized in terms of the angle ϕ. This degeneracy gives rise to a gapless mode in the spin wave spectra at zero temperature.

While the ground state energy is continuously degenerate the excitation spectra depend on the angle ϕ that characterizes the ground state spin configuration. This implies that the entropy and hence the free energy are not continuously degenerate, but instead manifest the fourfold symmetry of the underlying lattice. In the case of the pure dipolar system the fluctuations are such that the minima in the free energy have the spins aligned parallel to the lattice vectors [21]. This state is referred to as the AF1 state [24] or the columnar state [25]. This mechanism that stabilizes the formation of long range antiferromagnetic order at finite temperature is an example of the phenomenon known as 'order from disorder' [26].

Extending the pure dipolar model to include the isotropic exchange interaction does not lift the degeneracy of the dipolar ground state spin configurations and, in the case of an antiferromagnetic exchange interaction ($J < 0$), the continuously degenerate manifold of dipolar ground state spin configurations continues to define the ground state manifold for $|J| < 1.23g$ [24]. Monte Carlo simulations, however, show that the antiferromagnetic

[5] A sequence of two papers predicted that for low values of the ratio J/g the sequence of transitions would be from a perpendicular striped phase to planar ferromagnetic phase [20]. However, the sampling used in these calculations gave rise to a temperature dependent perpendicular anisotropy that affected the sequence of states observed at the reorientation transition.

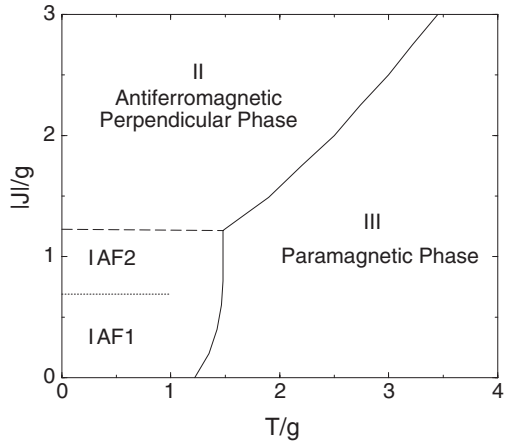

Figure 2. The JT phase diagram in the absence of the magnetic surface anisotropy $\kappa = 0$ from [24].

interaction does modify the character of the spin fluctuations such that the angle ϕ that characterizes the equilibrium spin configuration, switches from $\phi = 0$ to $\pi/4$ at $|J| \approx 0.7g$. This state is referred to as the AF2 state [24] or the microvortex state [25]. Originally it was postulated that this switch arose as a consequence of isolated spins being aligned perpendicular to the plane [24]. However, a similar dependence of the equilibrium spin configuration on the strength of the exchange constant has also been observed in simulations and linearized spin wave calculations for the planar X–Y model in which the spins are constrained to lie in the plane [27, 25].

For $|J| > 1.23g$ the ground state is given by the antiferromagnetic phase in which the spins are aligned perpendicular to the plane with each spin antiparallel to each of its nearest neighbours. We refer to this as the perpendicular phase. Simulations reveal that the phase boundary separating the planar AF2 phase and the perpendicular phase is almost independent of temperature and hence, while the transition is first order, the latent heat associated with the transition is extremely small [24]. The JT phase diagram for $J < 0$ and $\kappa = 0$ from [24] is shown in figure (2).

In this paper we present results from simulations which examine the interplay of the magnetic surface anisotropy and the dipolar anisotropy in the exchange dominated antiferromagnetic phase ($|J| > 1.23g$). In particular we present the κT phase diagram for $\kappa \leqslant 0$ and $J = -10g$. Of particular note is the prediction of a reorientation transition from the planar antiferromagnetic phase to the perpendicular antiferromagnetic phase with increasing temperature.

Results are reported for a several lattices sizes in the range $N = 32 \times 32$ to 104×104. Periodic boundary conditions are imposed on the spin configurations by constructing an infinite plane from replicas of a finite system. The summations of the dipolar interactions over the replicas is evaluated using the Ewald summation technique. The simulations are carried out using the standard Metropolis algorithm. For the results reported in the current work an equilibration time of 1×10^4 Monte Carlo steps/site (MCS/site) was used for each simulation, while the averaging was performed using samples taken every 10 MCS/site. The number of samples used to calculate the averages, however, depended on both the size of the system and the temperature. Therefore, our simulations are applied over a range from 10×10^4 MCS/site at high temperatures for the 104×104 system, to 29×10^4 MCS/site at low temperatures for the 32×32 system.

The layout of the paper is as follows. In the following section we define the order parameters for the perpendicular and planar phases of interest and present the results obtained from simulations. These results include the temperature dependence of the order parameters, the heat capacity and the energy, for $J = -10g$ and three values of κ. The data for $\kappa = -4.10g$ are shown to exhibit a reorientation transition from the planar antiferromagnetic phase to the perpendicular antiferromagnetic phase with increasing temperature. The κT phase diagram for $J = -10g$, constructed from the results from the Monte Carlo simulations, is presented and it is shown that the coexistence line separating the planar and the perpendicular phases satisfies an important thermodynamic relationship, analogous to the Clausius–Clapyron relation in fluids. An analysis of the low temperature magnetization is then presented, which suggests a softening of the spin wave spectra in the long wavelength limit close to the reorientation transition. We close the paper by summarizing the results and discussing their significance.

2. Magnetic properties

From figure 2 we see that, in the absence of the magnetic surface anisotropy, $\kappa = 0$, and choosing $J = -10g$ the ground state is the perpendicular antiferromagnetic state in which each spin is aligned perpendicular to the surface and antiparallel to each of its four nearest neighbours. We refer to this as the perpendicular antiferromagnetic phase. If we include a finite magnetic surface anisotropy, then the energy of this ground state spin configuration ($E_\perp$) is given by [28]

$$E_\perp = -2.6459g + 2J - \kappa. \tag{2}$$

If the magnetic surface anisotropy is such that it favours an in-plane orientation of the spins ($\kappa < 0$) then the ground state energy of the perpendicular antiferromagnetic phase increases as the strength of the magnetic surface anisotropy increases. At some critical value, which we denote by $-\kappa_0$, the perpendicular antiferromagnetic ground state will become unstable with respect to the planar antiferromagnetic phase, in which each spin is aligned parallel to the surface and antiparallel to each of its four nearest neighbours. The ground state energy of the planar antiferromagnetic phase ($E_\parallel$) is given by [28]

$$E_\parallel = 1.3229g + 2J. \tag{3}$$

Since the transition from the perpendicular to the planar antiferromagnetic phase occurs at $T = 0$ when

$$E_\perp = E_\parallel, \tag{4}$$

we obtain a value of κ_0 given by

$$\begin{aligned} \kappa_0 &= (2.646 + 1.323)g \\ &= 3.969g. \end{aligned} \tag{5}$$

To construct order parameters for these states we divide the lattice into four magnetic sublattices as described in the [24, 27]. Each magnetic sublattice is square with a lattice spacing twice that of the original lattice. The unit cell of the magnetic sublattice therefore contains four sites per unit cell, each site corresponding to one of the sublattices, which we denote by $\alpha \in \{1 \cdots 4\}$, as shown in figure 1. The sublattice magnetizations $\vec{M}_\perp^\alpha$ and $\vec{M}_\parallel^\alpha$ are then defined as

$$\vec{M}_\perp^\alpha = \frac{4}{N} \sum_{\vec{r}_\alpha} \sigma^z(\vec{r}_\alpha)\hat{z} \tag{6}$$

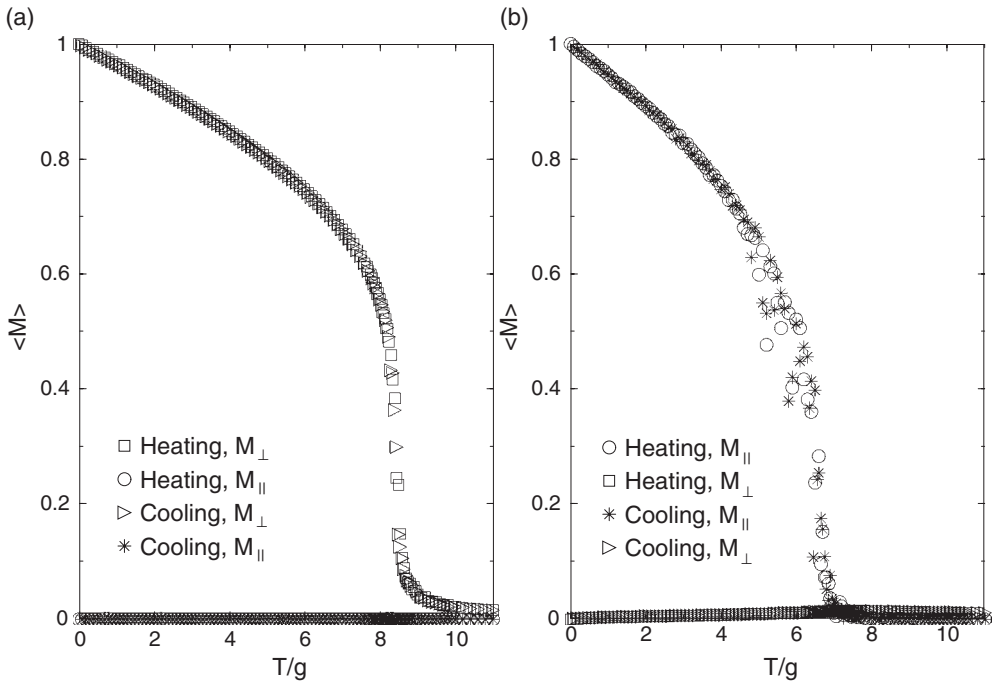

Figure 3. A plot of the two order parameters, $M_\perp$ and $M_\parallel$, as a function of both increasing and decreasing temperature for (a) $\kappa = -1.5g$ and (b) $\kappa = -7.0g$ for $L = 104$.

and

$$\vec{M}_\parallel^\alpha = \frac{4}{N}\left(\sum_{\vec{r}_\alpha} \sigma^x(\vec{r}_\alpha)\right)\hat{x} + \frac{4}{N}\left(\sum_{\vec{r}_\alpha} \sigma^y(\vec{r}_\alpha)\right)\hat{y} \tag{7}$$

from which we define the order parameters $M_\perp$ and $M_\parallel$ as

$$M_\perp = \tfrac{1}{4}\sum_{\alpha=1}^{4} |\vec{M}_\perp^\alpha| \tag{8}$$

$$M_\parallel = \tfrac{1}{4}|(M_x^1 + M_x^4 - M_x^3 - M_x^2)\hat{x} + (M_y^1 + M_y^4 - M_y^3 - M_y^2)\hat{y}|. \tag{9}$$

For the ground state of the perpendicular antiferromagnetic phase ($|\kappa| < \kappa_0$) we have

$$M_\perp = 1$$
$$M_\parallel = 0$$

while for the ground state of the planar antiferromagnetic phase ($|\kappa| > \kappa_0$) we have

$$M_\perp = 0$$
$$M_\parallel = 1.$$

The finite temperature order parameters are defined by the thermal averages of $M_\perp$ and $M_\parallel$ defined by equations (8) and (9) respectively. The temperature dependence of each of the two order parameters is shown in figures 3(a) and (b) as a function of both increasing and decreasing temperature for $\kappa = -1.5g$ and $\kappa = -7.0g$.

These two graphs show an antiferromagnetic ordered state at low temperature, a disordered state at higher temperature, and a continuous transition between them. For $\kappa = -1.5g$ the

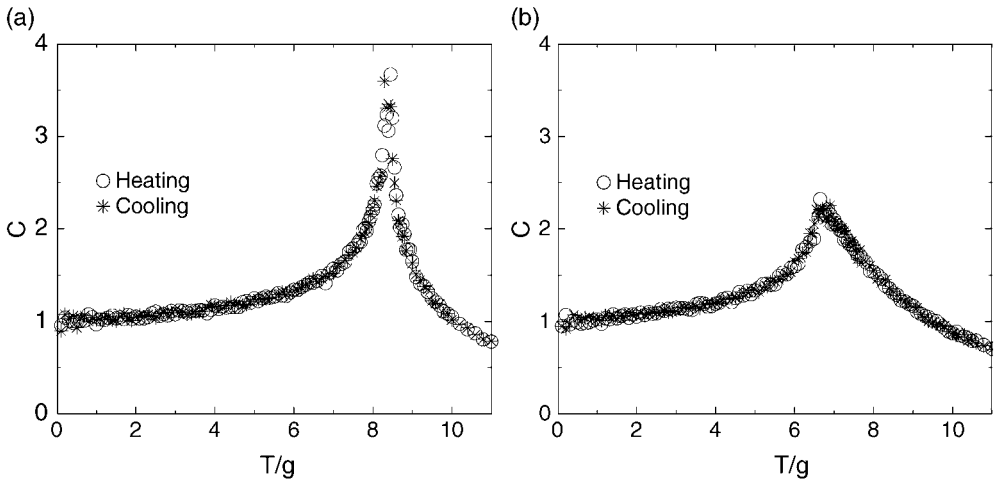

Figure 4. A plot of the heat capacity per spin as a function of both increasing and decreasing temperature for (a) $\kappa = -1.5g$ and (b) $\kappa = -7.0g$ for $L = 104$.

ground state is the perpendicular antiferromagnetic state. As the temperature is increased, figure 3(a) shows the perpendicular order parameter $M_\perp$ decreasing continuously, dropping rapidly to zero at around $T_N = (8.40 \pm 0.05)g$, while the planar order parameter $M_\parallel$ remains effectively zero. In contrast, for $\kappa = -7.0g$ the ground state is the planar antiferromagnetic state. As the temperature is increased, figure 3(b) shows the planar order parameter $M_\parallel$ decreasing continuously with increasing temperature, dropping rapidly to zero at around $T_N = (6.80 \pm 0.05)g$, while the perpendicular order parameter, $M_\perp$ remains effectively zero.

The existence of a continuous transition between the antiferromagnetic ordered state and the disordered state for both $\kappa/g = -1.5$ and $\kappa/g = -7.0$ is consistent with the absence of hysteresis in the two order parameters shown in figure 3. This is also in agreement with the data shown in figure 4 where the heat capacity of the system is plotted as a function of both increasing and decreasing temperature for $\kappa/g = -1.5$ (a) and for $\kappa/g = -7.0$ (b). The behaviour of the two order parameters and the heat capacity with temperature for $\kappa/g = -1.5$ and $\kappa/g = -7.0$ suggests that the system exhibits a second order transition between the perpendicular antiferromagnetic ordered state and the disordered state for low values of $|\kappa|$ ($|\kappa| < \kappa_0$), and a second order transition between the planar antiferromagnetic ordered state and the disordered state for large values of $|\kappa|$ ($|\kappa| > \kappa_0$).

The differences between magnetization and specific heat curves shown in figures 3 and 4 for the perpendicular phase $|\kappa/g| = 1.5$ and the planar phase $|\kappa/g| = 7.0$ in the vicinity of the transition to the paramagnetic phase merit further investigation. Some preliminary work evaluating the critical exponents for both the planar and perpendicular phases has been done; however, more detailed studies are required in order to determine the precise nature of the transition to the paramagnetic phase in each case.

The temperature dependence for the two order parameters $M_\parallel$ and $M_\perp$ are plotted as a function of temperature for $\kappa = -4.1g$. At $T = 0$ the system is in the planar phase with $M_\parallel = 1$ and $M_\perp = 0$. As the temperature is increased the data show that $M_\parallel$ decreases while $M_\perp$ remains effectively zero until $T_R \approx (1.42 \pm 0.02)g$, at which point the order parameters change over a very narrow temperature range with $M_\parallel$ dropping effectively to zero while $M_\perp$ increases to approximately 0.9. As the temperature is increased further, the system exhibits a

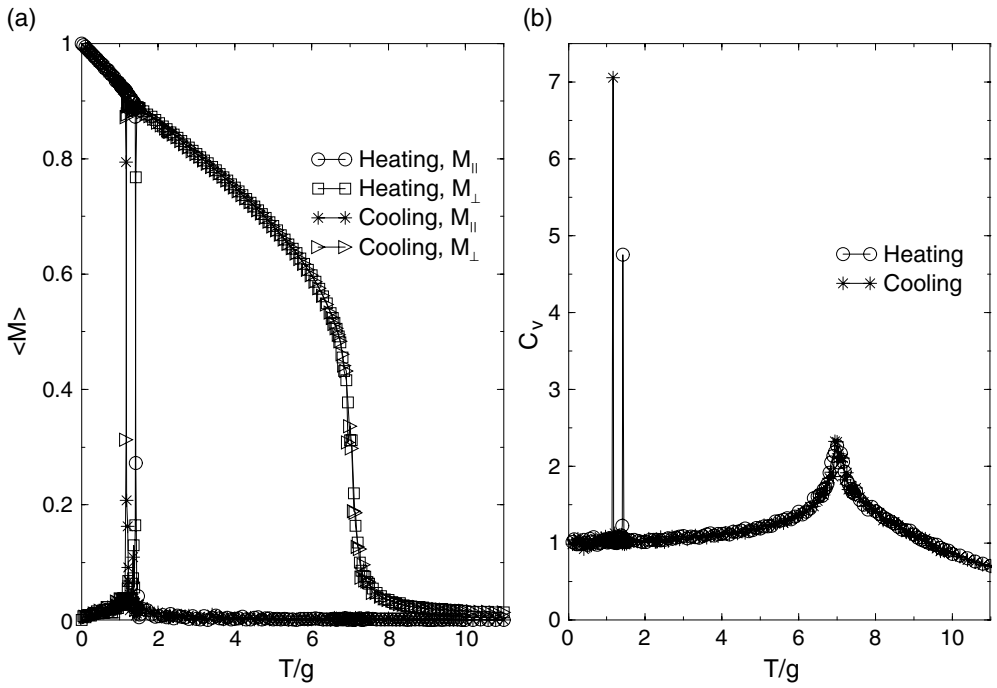

Figure 5. A plot of (a) the two order parameters, $M_\perp$ and $M_\parallel$, and (b) the heat capacity per spin as a function of both increasing and decreasing temperature for $\kappa = -4.1g$ with $L = 104$.

continuous transition to the paramagnetic phase at $T_{\rm N} = (7.05 \pm 0.05)g$. A similar behaviour is observed on cooling except that the abrupt change in the order parameter occurs at the slightly lower temperature $T_{\rm R} = (1.16 \pm 0.02)g$. The hysteresis at the transition is shown in more detail in figure 6, which shows the temperature dependence of the order parameters and the internal energy as a function of both increasing and decreasing temperature, in the vicinity of the reorientation transition. The change in the order parameters that occurs over a narrow range in temperature and which is observed in both heating and cooling corresponds to a reorientation transition.

This sequence of transitions is also reflected in the heat capacity data shown in figure 5(b), which shows three distinct peaks. The two narrow peaks correspond to the reorientation transition on heating and cooling, while the second broad peak corresponds to the transition from the perpendicular phase to the paramagnetic phase. This hysteresis, together with the almost discontinuous change in the order parameters and the very narrow peaks in the heat capacity, is consistent with a reorientation transition that is first order.

Further evidence regarding the nature of the reorientation transition is obtained from the xy conjugate field P_{xy} and the z conjugate field P_z defined as [24]

$$P(T)_{xy} = \frac{1}{N}\left\langle \sum_{\vec{R}} (\sigma_x^4 + \sigma_y^4) \right\rangle \tag{10}$$

$$P(T)_z = \frac{1}{N}\left\langle \sum_{\vec{R}} \sigma_z^2 \right\rangle. \tag{11}$$

It can be readily shown that at zero temperature $P_{xy} = 1$ and $P_z = 0$ for the planar phase, and $P_{xy} = 0$ and $P_z = 1$ for perpendicular phase, while in the disordered phase $P_{xy} = 2/5$ and

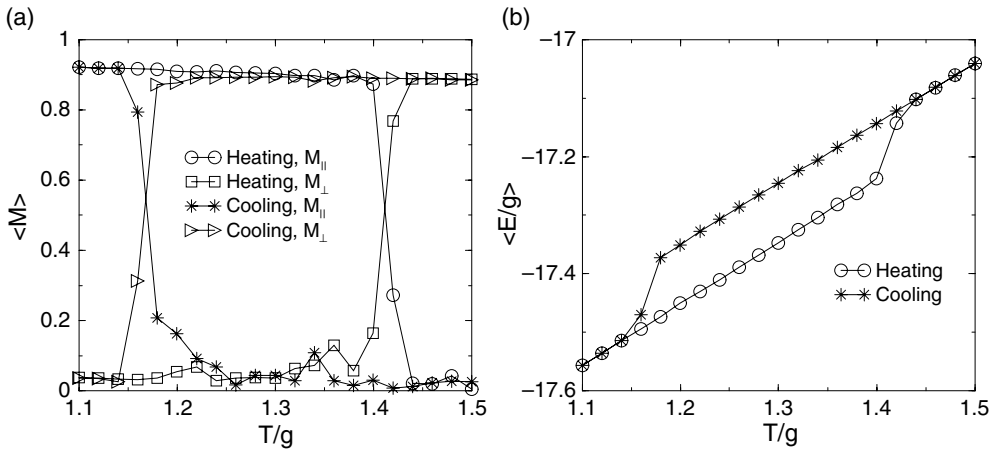

Figure 6. A plot of (a) the two order parameters, $M_\perp$ and $M_\parallel$, and (b) the total average internal energy per spin as a function of both increasing and decreasing temperature for $\kappa = -4.1g$ with $L = 104$.

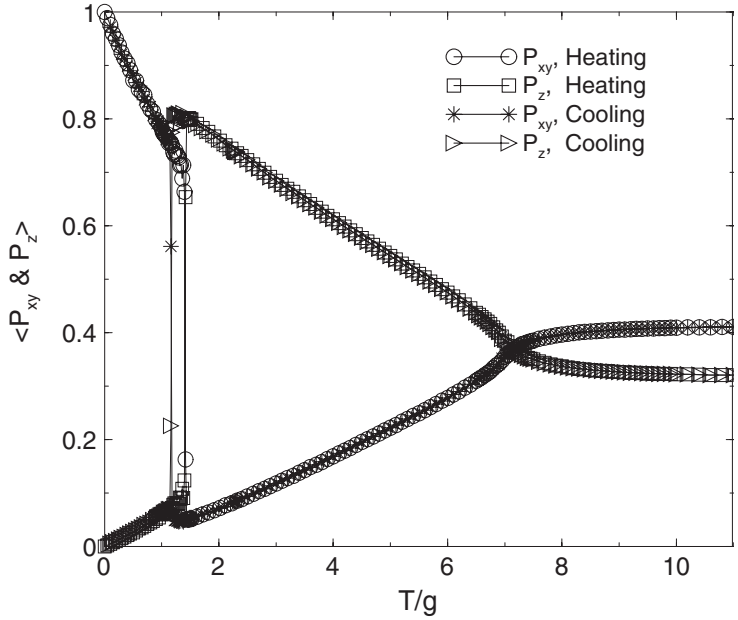

Figure 7. A plot of the two fields conjugate, P_{xy} and P_z, as a function of both increasing and decreasing temperature for $\kappa = -4.1g$ with $L = 104$.

$P_z = 1/3$. The temperature dependence of the two conjugate fields P_{xy} and P_z is shown in figure 7 for both increasing and decreasing temperature. Both exhibit an abrupt change over a very narrow range in temperature at the reorientation transition. At higher temperatures, P_{xy} extrapolates to $2/5$ and P_z extrapolates to $1/3$, indicating that the system is in the disordered phase at high temperature.

It is interesting to contrast the reorientation transition reported in this work for antiferromagnetic systems with that reported in the ferromagnetic case. While the complexities

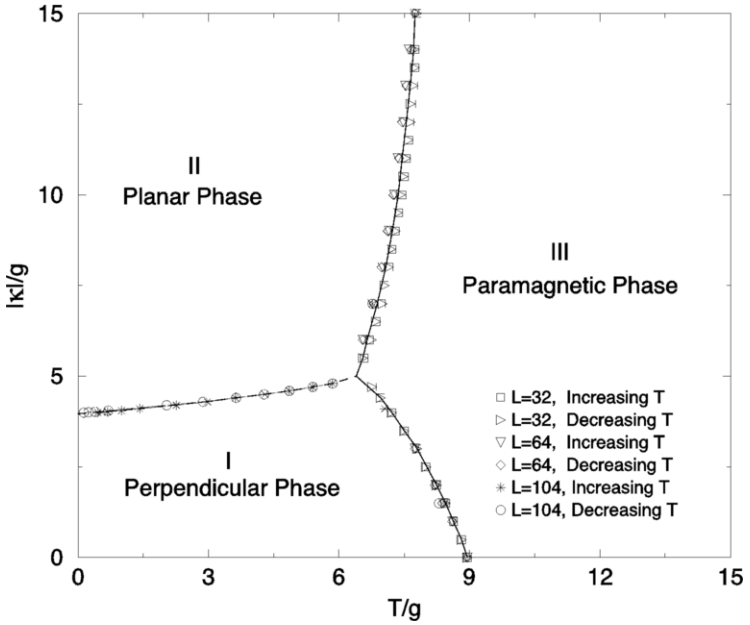

Figure 8. The phase diagram for the dipolar antiferromagnetic Heisenberg system with magnetic surface anisotropy as a function of $|\kappa|/g$ and T/g for $J = -10g$. Region I is the perpendicular antiferromagnetic phase, region II is the planar antiferromagnetic phase, and region III is the paramagnetic phase. The dashed line indicates first order transitions between the two ordered phases, while the two solid lines indicate second order transitions between the two ordered states and the disordered state.

arising from the inhomogenous striped phase have been noted, another important difference lies in the fact that the sequence of transitions for the ferromagnetic reorientation transitions is from a perpendicular phase at low temperature to a planar phase at high temperature [17, 18]. This contrasts with the results reported here, in which the sequence of transitions is from the planar phase at low temperature to the perpendicular phase at high temperature. However, the fact that the low temperature phase in both the ferromagnetic and the antiferromagnetic is stabilized by the magnetic surface anisotropy suggests that there are similarities between the two reorientation transitions that are not immediately apparent. At the most basic level both transitions may be understood qualitatively as a weakening of the strength of the magnetic surface anisotropy, relative to the dipolar interaction, by the thermal fluctuations.

3. The phase diagram

In figure 8, the results of the Monte Carlo simulations at finite temperature have been collected to form a phase diagram for both heating and cooling. This phase diagram shows three phase boundaries separating the perpendicular antiferromagnetic phase (region I), the planar antiferromagnetic phase (region II) and the paramagnetic phase (region III). The two solid lines indicate second order transitions between the two antiferromagnetic ordered states and the disordered state, while the dashed line is the phase boundary separating the two antiferromagnetic ordered phases.

If we assume, as the Monte Carlo data suggest, that the reorientation transition is indeed first order, and describe the coexistence line separating the perpendicular and the planar phases

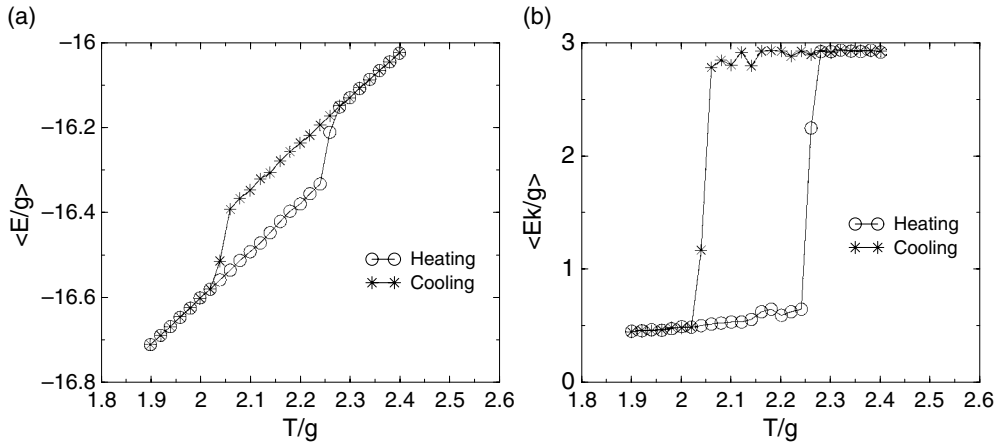

Figure 9. A plot of (a) the average internal energy per spin and (b) the average magnetic surface anisotropy energy per spin for $|\kappa| = 4.2g$ as a function of both increasing and decreasing temperature with $L = 104$.

by the function $\kappa_R(T)$, then the sequence of states observed at the transition on heating and cooling is determined by the fact that $d\kappa_R/dT > 0$. The slope of the coexistence can be expressed as

$$\frac{d\kappa_R}{dT} = \frac{\kappa \ell}{T_R \Delta E_\kappa} \tag{12}$$

where ℓ denotes the latent heat of the transition and ΔE_κ denotes the difference in the average anisotropy energy between the two equilibrium phases on the coexistence line. Figures 9(a) and (b) show how the total average internal energy (figure 9(a)) and the average anisotropy energy (figure 9(b)) change with increasing and decreasing temperature for $\kappa/g = -4.2$. From these data we estimate $T_R/g = 2.25 \pm 0.02$, $\ell/g = 0.142 \pm 0.003$, and $\Delta E_\kappa/g = 2.28 \pm 0.04$, which yields $d\kappa_R/dT = 0.116 \pm 0.013$ according to equation (12). By comparison, for $\kappa/g = -4.2$ estimates of κ_R from the coexistence line yield a slope $d\kappa_R/dT = 0.128 \pm 0.006$. This provides an useful consistency check on the results obtained from the simulations, in particular the slope of the coexistence line and hence the nature of the reorientation transition.

4. The temperature dependence of the order parameters in the limit $T \to 0$

The temperature dependence of the order parameters $M_\perp$ and $M_\parallel$ is shown in figures 10(a) and (b), for the range $0 < T/g < 1.5$ for several values of κ. The data show two interesting features. Firstly the order appears to decrease linearly with temperature, as one would expect on the basis of linearized spin wave theory, and secondly the magnitude of the slope $|dM/dT|$ increases as the reorientation transition is approached, for both the perpendicular and the planar phase, suggesting a softening of the spin wave spectra close to the transition.

Figure 11 shows a comparison between the slope $\lim_{T\to 0} |dM_\perp/dT|$ as a function of κ for both $|\kappa| < \kappa_0$ and $|\kappa| > \kappa_0$, obtained from the data shown in figure 10. Also shown in figure 11 is the phenomenological relationship

$$\lim_{T\to 0} \left| \frac{dM}{dT} \right| = \frac{a}{|b - (|\kappa|/g)^c|^d}, \tag{13}$$

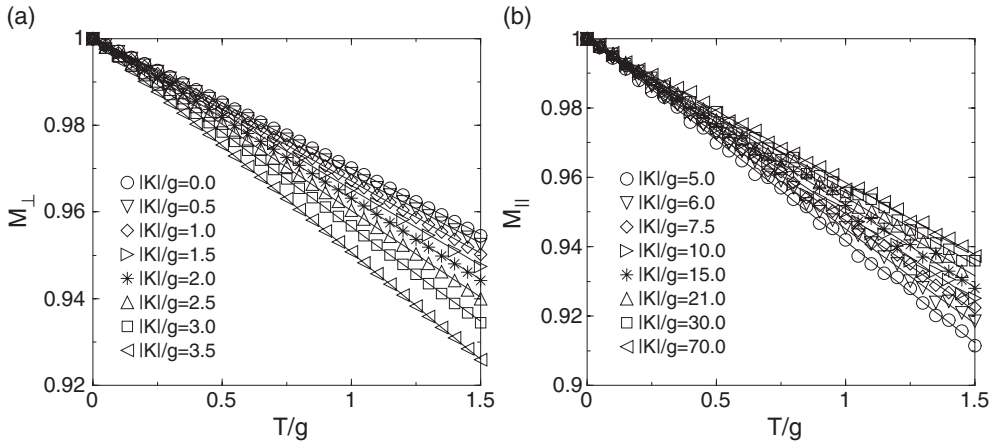

Figure 10. A plot of (a) the perpendicular order parameter $M_\perp$ for several values of $|\kappa| < |\kappa|_0$ and (b) the planar order parameter $M_\parallel$, for several values of $|\kappa| > |\kappa|_0$ as a function of increasing temperature with $L = 104$.

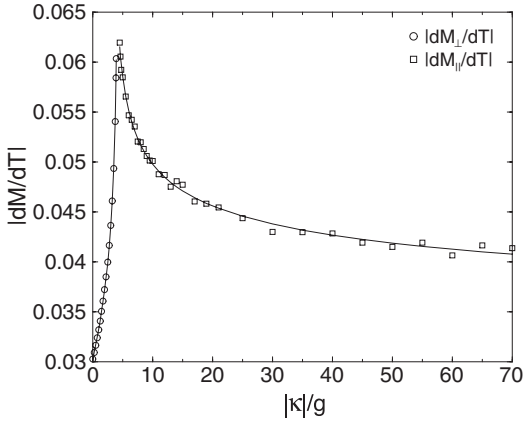

Figure 11. A plot of the slope $\lim_{T\to 0} \mathrm{d}M_\perp/\mathrm{d}T$ and the slope $\lim_{T\to 0} \mathrm{d}M_\parallel/\mathrm{d}T$ as a function of $|\kappa|/g$.

where the coefficients a, b, c and d are determined by a separate regression analysis for $|\kappa| < \kappa_0$ and $|\kappa| > \kappa_0$. For $|\kappa| < \kappa_0$ the regression analysis yields the following estimates: $a = 0.0417$, $b = 3.2553$, $c = 0.7975$ and $d = 0.2762$. This relationship predicts that the slope of the $M_\perp$ order parameter diverges at $|\kappa|/g = 4.3930$, which lies just above κ_0. For $|\kappa| > \kappa_0$, the regression analysis yields the following estimates: $a = 0.0498$, $b = 1.7385$, $c = 0.4385$ and $d = 0.1293$. This relation predicts that the slope of the $M_\parallel$ order parameter diverges at $|\kappa|/g = 3.5296$, which lies just below κ_0.

While the data reported here are all for $L = 104$, a comparison of the results obtained for smaller systems ($L = 64, 32$) shows that the results are insensitive to the size of the system. This suggests that the singular nature of the phenomenological relation given in equation (13) is not an artefact of the finite size of the system. It would be useful therefore to compare the results reported in this study with the low temperature magnetization calculated from spin wave theory for both the perpendicular and planar phases. The results from such a calculation

might also provide some useful insight into the mechanism driving the reorientation transition in these systems.

5. Conclusion

The results from a series of Monte Carlo simulations of the classical Heisenberg model on a square lattice were presented, in which the energy for a given spin configuration was given by the sum of an antiferromagnetic exchange interaction, the dipolar interaction and the magnetic surface anisotropy. Choosing $J = -10g$, the relevant states are antiferromagnetic in which every spin is aligned in the opposite direction to its neighbours. The orientation of the antiferromagnetic state is determined by the strength of the dipolar interaction, which favours the perpendicular antiferromagnetic phase, and the magnetic surface anisotropy, which, for $\kappa < 0$, favours the planar antiferromagnetic state.

Simulations for small values of $|\kappa|$ show a finite perpendicular antiferromagnetic order parameter which decreases with increasing temperature until the system undergoes a second order phase transition to the paramagnetic phase at the Néel temperature, at which point the order parameter is effectively zero. A similar behaviour is observed for large values of $|\kappa|$, with the difference that the ordered phase is the planar phase.

For intermediate values of κ there exists a narrow range around $|\kappa| \approx \kappa_0$ for which the system undergoes a reorientation transition from the planar to the perpendicular phase with increasing temperature. The almost discontinuous change in the order parameters, the very narrow peak in the specific heat, and the hysteresis observed in the Monte Carlo data at the reorientation transition all indicate that it is a first order transition. As the temperature is further increased the system undergoes a second order transition to the paramagnetic phase. These results are summarized in the phase diagram presented in figure 8.

While the sequence of phases observed in the reorientation transition in the antiferromagnetic case is the opposite to that observed for the ferromagnetic case, both may be qualitatively understood as a reduction in the strength of the magnetic surface anisotropy relative to the dipolar interaction, due to the thermal fluctuations.

It was also noted that, despite the apparent first order nature of the reorientation transition, the low temperature magnetization reveals a softening of the spin wave spectra close to the transition.

While the prediction of the reorientation transition in antiferromagnetic thin films is perhaps the most interesting result to emerge from these studies, the results presented in this paper together with the results presented in [24] and [27, 25] provide a fairly comprehensive picture of the magnetic phase behaviour of antiferromagnetic films.

Acknowledgments

This work was supported in part by the Natural Sciences and Engineering Research Council of Canada. The authors thank Memorial University of Newfoundland and the University of Calgary for the use of computational resources, provided under the auspices of C3.ca.

References

[1] Prinz G A 1998 *Science* **282** 1660
[2] Wolf S A, Awschalom D D, Buhrman R A, Daughton J M, Molnar S v, Roukes M L, Chtchelkanova A Y and Treger D M 2001 *Science* **294** 1488
[3] Cowburn R P, Adeyeye A O and Welland M E 1999 *New J. Phys.* **1** 6711

[4] Giersig M and Hilgendorff M 1999 *J. Phys. D: Appl. Phys.* **32** L111
[5] Cowburn R P 1999 *J. Phys. D: Appl. Phys.* **33** R1
[6] Brown S E, Thompson J D, Willis J O, Aikin R M, Zirngiebel E, Smith J L, Fisk Z and Scwarz R B 1987 *Phys. Rev.* B **36** 2298
[7] Lynn J W, Clinton T W, Li W-H, Erwin R W, Liu J Z, Shelton R N and Klavins P 1990 *J. Appl. Phys.* **67** 4533
[8] Clinton T W, Lynn J W, Liu J Z, Jia Y X and Shelton R N 1991 *J. Appl. Phys.* **70** 5751
[9] Simizu S, Bellesis G H, Lukin J, Friedberg S A, Lessure H S, Fine S M and Greenblatt M 1989 *Phys. Rev.* B **39** 9099
[10] Dunlap B D, Slaski M, Sungaila Z, Hinks D G, Zhang K, Segre C, Malik S K and Alp E E 1988 *Phys. Rev.* B **37** 592
[11] Male'ev S V 1976 *Sov. Phys.—JETP* **43** 1240–6
[12] Garel T and Doniach S 1982 *Phys. Rev.* B **26** 325–9
[13] Kaplan B and Gehring G A 1993 *J. Magn. Magn. Mater.* **128** 111–6
[14] MacIsaac A B, Whitehead J P, Robinson M C and De'Bell K 1995 *Phys. Rev.* B **51** 16033–45
Booth I, MacIsaac A B, Whitehead J P and De'Bell K 1995 *Phys. Rev. Lett.* **75** 950–3
[15] Pappas D P, Kamper K-P and Hopster H 1990 *Phys. Rev. Lett.* **64** 3179
[16] Allenspach R, Stampanoni M and Bischof A 1990 *Phys. Rev. Lett.* **65** 3344–7
[17] Chui S T 1994 *Phys. Rev.* B **50** 12559
[18] Hucht A, Moschel A and Usadel K D 1995 *J. Magn. Magn. Mater.* **481** 32
[19] Hucht A and Usadel K D 1997 *Phys. Rev.* B **55** 12309
[20] MacIsaac A B, Whitehead J P, De'Bell K and Poole P H 1996 *Phys. Rev. Lett.* **77** 739
MacIsaac A B, De'Bell K and Whitehead J P 1998 *Phys. Rev. Lett.* **80** 616
[21] De'Bell K, MacIsaac A B, Booth I N and Whitehead J P 1997 *Phys. Rev.* B **55** 15108–18
[22] Carbognani A, Rastelli E, Regina S and Tassi A 2000 *Phys. Rev.* **62** 1015
[23] Zimmerman G O, Ibrahim A K and Wu F Y 1988 *Phys. Rev.* **37** 2059
[24] Abu-Labdeh A M, Whitehead J P, De'Bell K and MacIsaac A B 2001 *Phys. Rev.* B **65** 024434
[25] Rastelli E, Regina S, Tassi A and Carbognani A 2002 *Phys. Rev.* B **65** 94412
[26] Henley C 1989 *Phys. Rev. Lett.* **62** 2056–9
Prakash S and Henley C L 1990 *Phys. Rev.* B **42** 6574–89
[27] Abu-Labdeh A M, Whitehead J P, De'Bell K and MacIsaac A B 2002 *J. Phys.: Condens. Matter* **14** 7155
[28] De'Bell K, MacIsaac A B and Whitehead J P 2000 *Rev. Mod. Phys.* **72** 225